

Context-aware surrogate modeling for balancing approximation and sampling costs in multi-fidelity importance sampling and Bayesian inverse problems

Terrence Alsup*

Benjamin Peherstorfer*

October 2020

Multi-fidelity methods leverage low-cost surrogate models to speed up computations and make occasional recourse to expensive high-fidelity models to establish accuracy guarantees. Because surrogate and high-fidelity models are used together, poor predictions by the surrogate models can be compensated with frequent recourse to high-fidelity models. Thus, there is a trade-off between investing computational resources to improve surrogate models and the frequency of making recourse to expensive high-fidelity models; however, this trade-off is ignored by traditional modeling methods that construct surrogate models that are meant to replace high-fidelity models rather than being used together with high-fidelity models. This work considers multi-fidelity importance sampling and theoretically and computationally derives the optimal trade-off between improving the fidelity of surrogate models for constructing more accurate biasing densities and the number of samples that is required from the high-fidelity model to compensate poor biasing densities. Numerical examples demonstrate that such optimal—context-aware—surrogate models for multi-fidelity importance sampling have lower fidelity than what typically is set as tolerance in traditional model reduction, leading to runtime speedups of up to one order of magnitude in the presented examples.

Keywords: Multi-fidelity, importance sampling, Bayesian inverse problem, chi-squared divergence, Monte Carlo

1 Introduction

Surrogate models provide low-cost approximations of computationally expensive high-fidelity models and so are widely used to make tractable a variety of outer-loop applications such as control, optimization, and uncertainty quantification [30]. Typical examples of surrogate models are simplified-physics models [26, 24, 5], data-fit and machine-learning models [14, 32], and projection-based reduced models [2, 31, 3, 17, 8]. Multi-fidelity methods combine surrogate models for speedups and high-fidelity models for accuracy guarantees [30, 25]. Recourse to the high-fidelity model enables compensation for poor surrogate accuracy, in stark contrast to traditional single-fidelity methods that use surrogate models alone. The opportunity of multi-fidelity methods that we exploit in the following is that it is unnecessary that surrogate models achieve tight

*Courant Institute of Mathematical Sciences, New York University (alsup@cims.nyu.edu, pehersto@cims.nyu.edu)

accuracy guarantees because high-fidelity models are occasionally evaluated to correct results. Rather, it can be beneficial to use surrogate models with very low accuracy in favor of very cheap training and evaluation costs. Clearly, there is a limit of how low the accuracy of surrogate models can be in favor of costs before surrogate models become useless. Thus, there is a trade-off between increasing the accuracy of surrogate models with expensive training methods versus making more frequent recourse to the expensive high-fidelity model to compensate less accurate, but cheaper, surrogate models. Surrogate models that exploit this trade-off are called context-aware models [27]. This work derives context-aware surrogate models for multi-fidelity importance sampling [28], where the surrogate model is used for constructing the Laplace approximation as biasing density. Our numerical results show that such context-aware surrogate models for multi-fidelity importance sampling can achieve an error reduction of more than one order of magnitude compared to using a single model alone.

We review related literature. First, there is work on adaptive discretizations for multi-level Monte Carlo methods and stochastic collocation methods [18, 19, 20] that adaptively refine meshes and time steps to obtain a non-uniform hierarchy of surrogate models. Additionally, there is work on continuous multi-level Monte Carlo [12] that adapts the model hierarchy in a non-uniform fashion. In contrast to coarse-grid discretizations, we will consider surrogate models for constructing biasing densities, which incurs training (offline) costs that we trade off with surrogate-model fidelity and frequency of recourse to the high-fidelity model. The work [9] learns data-fit surrogate models for solving Bayesian inverse problems, without building on multi-fidelity methods and thus without deriving the trade-off between model accuracy and costs. Second, the works [27, 13] explore the trade-off between surrogate-model fidelity and number of times to make recourse to the high-fidelity for multi-fidelity Monte Carlo estimation with control variates, which is in contrast to using importance sampling for variance reduction as in this work. In [10], the authors consider local, data-fit approximations and balance the decay rate of the bias due to the approximation with the variance of sampling with Markov chain Monte Carlo methods. Third, there is a large body of work on using surrogate models and multi-fidelity methods that build on importance sampling without explicitly exploiting the trade-off given by surrogate-model fidelity and frequency of recourse to the high-fidelity model. The work [23, 22] develops a principled strategy to switch between sampling from a surrogate model and from the high-fidelity model to speedup failure and rare event probability estimation. In [7], the authors build on *a posteriori* error estimators to decide if either a surrogate model or the high-fidelity model is evaluated. The authors of [28] introduce a multi-fidelity method for importance sampling. In the first step, the biasing density is constructed with the surrogate model. In the second step, samples are drawn from the biasing density and the estimate is derived with the high-fidelity model. The authors of [16, 15] develop a multi-fidelity method for importance sampling to efficiently estimate risk-measures such as the conditional value-at-risk.

We build further on the the multi-fidelity importance sampling idea [28] of computing biasing densities with surrogate models. In particular, we develop bounds of the error of multi-fidelity importance sampling that depends on the surrogate-model fidelity and then derive the optimal trade-off between surrogate-model fidelity and computational costs. The first key ingredient is that we use the Laplace approximation computed with the surrogate model as biasing density. The quality of Laplace approximations has been studied in [11] in terms of the Kullback-Leibler (KL) divergence and in [34] in terms of the Hellinger distance when the noise level approaches zero. Instead, we consider the χ^2 divergence [37] due to its natural interpretation as the variance of the importance weights. The second key ingredient is bounding the error of the importance sampling estimator such as introduced in [6, 1, 33]. These error bounds take the form of a probability divergence between the target distribution and the biasing distribution, which we will use to separate the error due to sampling and the error due to the quality of the biasing density that corresponds to the surrogate-model fidelity.

This manuscript is structured as follows. In Section 2 we outline importance sampling in the multi-fidelity

setting along with the bound on the mean-squared error (MSE) in terms of the χ^2 divergence as presented in [1]. Section 3 is the main contribution of this work and derives a bound on the χ^2 divergence from the target to the biasing distribution in terms of the surrogate-model fidelity that leads to the formulation of the optimization problem for the optimal fidelity. In deriving this bound, we make use of the notion of sub-Gaussian distributions [38] in Section 3.1. In Section 4, we apply the results from Section 3 in the case where the target distribution is a posterior distribution arising from a Bayesian inverse problem. In Section 5, we demonstrate our method on two numerical examples. Multi-fidelity importance sampling with context-aware (optimally traded off) surrogate models achieve more than one order of magnitude error reduction compared to traditional importance sampling that uses the high-fidelity model alone with the same costs.

2 Importance sampling and problem formulation

Section 2.1 describes the setup of our problem. Section 2.2 is a brief overview of importance sampling and Section 2.3 overviews how the quality of a biasing density influence importance sampling estimators in terms of the χ^2 divergence. Section 2.4 illustrates the multi-fidelity approach to importance sampling and Section 2.5 formulates the optimal trade-off problem that we are interested in.

2.1 Notation and problem setting

Let $(\Theta, \mathcal{B}(\Theta), p)$ denote a probability space where $\Theta \subseteq \mathbb{R}^d$ is the domain for parameters θ , $\mathcal{B}(\Theta)$ is the Borel σ -algebra of Θ , and p is a probability distribution on Θ . Let p be absolutely continuous with respect to the Lebesgue measure on \mathbb{R}^d and refer to both the measure and the density function as p . Furthermore, the density p may only be known up to a normalizing constant $p = \frac{1}{Z}\tilde{p}$, where $\tilde{p} \geq 0$ is the un-normalized density and $Z = \int_{\Theta} \tilde{p}(\theta) d\theta$ is the normalizing constant. The density p and the un-normalized density \tilde{p} are expensive to evaluate. The goal is to compute a quantity of interest (QoI) that takes the form of an expectation

$$\mathbb{E}_p[f] = \int_{\Theta} f(\theta)p(\theta) d\theta, \quad (1)$$

where f is a bounded measurable test function (i.e. $\|f\|_{L^\infty} < \infty$ where $\|f\|_{L^\infty} = \text{ess sup}_{\theta \in \Theta} |f(\theta)|$ under the measure p).

2.2 Importance sampling

Let q be another probability distribution on the Borel space $(\Theta, \mathcal{B}(\Theta))$ that is absolutely continuous with respect to the Lebesgue measure on \mathbb{R}^d and is such that p is absolutely continuous with respect to q . We let q refer to both the probability distribution and the density function with respect to the Lebesgue measure. If sampling directly from p is impossible and the normalizing constant Z is unknown, then self-normalized importance sampling can be used with q as the biasing distribution to estimate the expectation (1). Draw m independent and identically distributed samples $\{\theta^{(i)}\}_{i=1}^m \stackrel{\text{i.i.d.}}{\sim} q$ from the biasing distribution q and re-weight with the target distribution p to obtain the self-normalized importance sampling estimator

$$\hat{f}_m = \frac{\sum_{i=1}^m f(\theta^{(i)})w(\theta^{(i)})}{\sum_{i=1}^m w(\theta^{(i)})} \quad (2)$$

of $\mathbb{E}_p[f]$, where the importance weights $w(\theta^{(i)})$ are given by evaluating the likelihood ratio $w(\theta) = \frac{p(\theta)}{q(\theta)}$ at the samples $\theta^{(i)}$. The estimator (2) is a consistent estimator of $\mathbb{E}_p[f]$ as the sample size $m \rightarrow \infty$.

2.3 Error of the importance sampling estimator

Theorem 2.1 of [1] gives the following bound on the mean-squared error (MSE) of the self-normalized importance sampling estimator (2): if p is absolutely continuous with respect to q and $\mathbb{E}_q[w^2] < \infty$, then

$$\mathbb{E} \left[\left(\hat{f}_m - \mathbb{E}_p[f] \right)^2 \right] \leq \frac{4\|f\|_{L^\infty}^2}{m} (\chi^2(p \parallel q) + 1) \quad (3)$$

holds, with the χ^2 squared divergence from p to q defined as

$$\chi^2(p \parallel q) + 1 = \text{Var}_q \left[\frac{p}{q} \right] + 1 = \int_{\Theta} \left(\frac{p(\boldsymbol{\theta})}{q(\boldsymbol{\theta})} \right)^2 q(\boldsymbol{\theta}) d\boldsymbol{\theta} = \int_{\Theta} \frac{p(\boldsymbol{\theta})}{q(\boldsymbol{\theta})} p(\boldsymbol{\theta}) d\boldsymbol{\theta}. \quad (4)$$

Since f is bounded, it holds $(\hat{f}_m - \mathbb{E}_p[f])^2 \leq 4\|f\|_{L^\infty}^2$, which means that the bound (3) is only useful if $m \geq \chi^2(p \parallel q) + 1$. The worst case constant 4 in (3) is attained when $f - \mathbb{E}_q[f] = 2\|f\|_{L^\infty}$ q -almost everywhere. The bound (3) motivates setting the effective sample size to

$$m_{\text{eff}} = \frac{m}{\chi^2(p \parallel q) + 1}, \quad (5)$$

so that a large χ^2 divergence corresponds to a large variance of the weights, meaning more samples are needed to reduce the MSE of the estimator (2). The effective sample size (5) motivates finding a biasing density q that is close to p with respect to the χ^2 divergence. Note that the χ^2 divergence is related to other probability divergences such as the Kullback-Leibler (KL) divergence

$$\text{KL}(p \parallel q) = \int_{\Theta} \log \left(\frac{p(\boldsymbol{\theta})}{q(\boldsymbol{\theta})} \right) p(\boldsymbol{\theta}) d\boldsymbol{\theta}$$

and the Hellinger distance

$$d_H(p, q) = \left(\frac{1}{2} \int_{\Theta} \left(\sqrt{p(\boldsymbol{\theta})} - \sqrt{q(\boldsymbol{\theta})} \right)^2 d\boldsymbol{\theta} \right)^{1/2}.$$

The relation is a lower bound given by Jensen's inequality

$$e^{2d_H(p, q)^2} \leq e^{\text{KL}(p \parallel q)} \leq \chi^2(p \parallel q) + 1,$$

see [37] for more general information regarding these probability divergences.

2.4 Finding a biasing density

Let $(\Theta, \mathcal{B}(\Theta), p_h)$ be a sequence of probability spaces, where the distributions p_h are approximations to p and the index $h > 0$ denotes the fidelity of the approximation. For each h , let p_h be absolutely continuous with respect to the Lebesgue measure on \mathbb{R}^d and use p_h to denote both the density function and the distribution. Let the density functions converge pointwise so $p_h(\boldsymbol{\theta}) \rightarrow p(\boldsymbol{\theta})$ as $h \rightarrow 0$ for every $\boldsymbol{\theta} \in \Theta$. Define $C_{\text{hi}} > 0$ as the cost of evaluating the un-normalized high-fidelity density \tilde{p} and $c(h) > 0$ as the cost of evaluating the un-normalized surrogate density \tilde{p}_h . The surrogate densities p_h can be used instead of p to find a biasing density q_h resulting in the multi-fidelity importance sampling (MFIS) [28] estimator

$$\hat{f}_{h,m} = \frac{\sum_{i=1}^m f(\boldsymbol{\theta}^{(i)}) w_h(\boldsymbol{\theta}^{(i)})}{\sum_{i=1}^m w_h(\boldsymbol{\theta}^{(i)})} \quad \text{where} \quad \{\boldsymbol{\theta}^{(i)}\}_{i=1}^m \stackrel{\text{i.i.d.}}{\sim} q_h, \quad (6)$$

of $\mathbb{E}_p[f]$ with the importance weights $w_h = \tilde{p}/\tilde{q}_h$ given by the ratio of the un-normalized densities \tilde{p} and \tilde{q}_h . The bound (3) shows that the quality of the biasing density with respect to the MSE is determined by the variance of the weights w_h and thus that the number of samples needed to achieve an error tolerance depends directly on the fidelity h of the approximation.

2.5 Problem formulation

Multi-fidelity importance sampling gives rise to the following two-step process of estimating $\mathbb{E}_p[f]$: (i) finding the biasing density q_h from p_h and (ii) evaluating the un-normalized densities \tilde{q}_h and \tilde{p} at m samples to obtain an estimate (6) of $\mathbb{E}_p[f]$. The first step incurs *training* costs $c^{\text{train}}(h)$ to derive q_h using p_h and the second step incurs *online* costs of evaluating the un-normalized surrogate and expensive high-fidelity densities. The two steps give rise to a trade-off; investing high training costs to find a good biasing density that keeps the χ^2 divergence low means that few evaluations of the expensive high-fidelity density are required in the online step and vice versa. Traditional model reduction [31, 3, 31] typically targets computations where the surrogate model replaces the high-fidelity, where such a trade-off does not exist. Thus, traditional model reduction provides little guidance on the mathematical formulation of this trade-off and solving for the corresponding optimal fidelity.

3 Context-aware surrogate models for multi-fidelity importance sampling

We consider the following trade-off: given an error tolerance ϵ , what is the optimal fidelity h of the surrogate model that minimizes the total computational costs subject to the mean-squared error of the multi-fidelity importance sampling estimator (6) being below or equal to the tolerance ϵ . We refer to surrogate models with optimally selected fidelity in multi-fidelity methods as *context-aware* because the fidelity is determined specifically for the online computations of the problem (context) at hand [27], rather than being prescribed without taking the specific context of multi-fidelity computations into account as in traditional model reduction [31, 3, 31].

Section 3.1 introduces the notion of a sub-Gaussian distribution which is used in Section 3.2 to derive an upper bound for $\chi^2(p \parallel q_h)$ that depends on h . Section 3.3 introduces the Laplace approximation q_h of the low-fidelity density p_h to be used as the biasing density and Section 3.4 uses the bound on the χ^2 divergence to formulate an optimization problem for the optimal fidelity h^* . Section 3.5 summarizes the entire computational procedure in algorithmic form.

3.1 Sub-Gaussian distributions

For importance sampling, it is imperative that the importance weights have finite variance (i.e., finite χ^2 divergence) which means that the tails of the biasing density cannot be significantly lighter than the tails of the target density p . Sub-Gaussian distributions are characterized by their fast tail decay. A useful norm for quantifying the tail decay of a real-valued random variable is the Orlicz norm defined as

$$\|x\|_{\psi_2} = \inf \{t > 0 \mid \mathbb{E} [\exp(x^2/t^2)] \leq 2\} ,$$

see [38, Sec. 2.5, Sec. 3.4] for other equivalent definitions. For a real random vector $\mathbf{x} = (x_1, \dots, x_d)$, the Orlicz norm is defined to be

$$\|\mathbf{x}\|_{\psi_2} = \sup_{\mathbf{v} \in S^{d-1}} \|\mathbf{v}^T \mathbf{x}\|_{\psi_2} ,$$

where $S^{d-1} \subset \mathbb{R}^d$ is the unit sphere defined as $S^{d-1} = \{\mathbf{v} \in \mathbb{R}^d : \|\mathbf{v}\|_2 = 1\}$. A probability distribution π is said to be sub-Gaussian if any random variable $\mathbf{x} \sim \pi$ has $\|\mathbf{x}\|_{\psi_2} < \infty$. Two examples of sub-Gaussian distributions are multivariate Gaussians and distributions with compact support. If $\mathbf{x} \sim N(0, \sigma^2 \mathbf{I})$ then $\|\mathbf{x}\|_{\psi_2} = \sigma$. In the following Lemma 1 we give a characterization of sub-Gaussian distributions that will be used in the following sections. The lemma is a multi-dimensional version of Proposition 2.5.2 (iv) in [38]. We did not find this specific result in the literature.

Lemma 1. *A random vector \mathbf{x} with density π is sub-Gaussian if and only if there exists a symmetric positive-definite matrix \mathbf{A} such that for all vectors $\boldsymbol{\mu} \in \mathbb{R}^d$*

$$\mathbb{E}_\pi [\exp ((\mathbf{x} - \boldsymbol{\mu})^T \mathbf{A} (\mathbf{x} - \boldsymbol{\mu}))] < \infty .$$

Proof. Suppose that \mathbf{x} is a sub-Gaussian random vector and consider the matrix to be a multiple of the identity, $\mathbf{A} = \alpha \mathbf{I}$ with $\alpha > 0$. We now only need to show that there exists an $\alpha > 0$ such that for all $\boldsymbol{\mu} \in \mathbb{R}^d$

$$\mathbb{E}_\pi [\exp (\alpha \|\mathbf{x} - \boldsymbol{\mu}\|^2)] = \mathbb{E}_\pi [\exp ((\mathbf{x} - \boldsymbol{\mu})^T \mathbf{A} (\mathbf{x} - \boldsymbol{\mu}))] < \infty .$$

Since $\|\mathbf{v} + \mathbf{w}\|^2 \leq 2\|\mathbf{v}\|^2 + 2\|\mathbf{w}\|^2$ by the triangle inequality and the fact that $(a + b)^2 \leq 2a^2 + 2b^2$, we get the upper bound

$$\mathbb{E}_\pi [\exp (\alpha \|\mathbf{x} - \boldsymbol{\mu}\|^2)] \leq \mathbb{E}_\pi [\exp (2\alpha \|\boldsymbol{\mu}\|^2 + 2\alpha \|\mathbf{x}\|^2)] = \exp (2\alpha \|\boldsymbol{\mu}\|^2) \mathbb{E}_\pi [\exp (2\alpha \|\mathbf{x}\|^2)] .$$

Therefore, we only need to find $\alpha > 0$ such that

$$\mathbb{E}_\pi [\exp (2\alpha \|\mathbf{x}\|^2)] < \infty .$$

We now use the assumption that \mathbf{x} is sub-Gaussian by taking the marginals

$$\begin{aligned} \mathbb{E}_\pi [\exp (2\alpha \|\mathbf{x}\|^2)] &= \mathbb{E}_\pi \left[\exp \left(2\alpha \sum_{i=1}^d x_i^2 \right) \right] \\ &= \mathbb{E}_\pi \left[\exp \left(2\alpha \sum_{i=1}^d |\mathbf{e}_i^T \mathbf{x}|^2 \right) \right] \\ &= \mathbb{E}_\pi \left[\prod_{i=1}^d \exp (2\alpha |\mathbf{e}_i^T \mathbf{x}|^2) \right] , \end{aligned}$$

where \mathbf{e}_i is the i -th canonical unit vector. We now proceed by induction on the dimension d and repeatedly use the Cauchy-Schwarz inequality to show that this expectation is finite. When $d = 1$, take α_1 such that $\frac{1}{\sqrt{2\alpha_1}} > \|\mathbf{x}\|_{\psi_2}$ so that

$$\mathbb{E}_\pi [\exp (2\alpha_1 |\mathbf{e}_1^T \mathbf{x}|^2)] = \mathbb{E}_\pi \left[\exp \left(\frac{|\mathbf{e}_1^T \mathbf{x}|^2}{(1/\sqrt{2\alpha_1})^2} \right) \right] \leq 2 .$$

Note that since \mathbf{x} is sub-Gaussian $\|\mathbf{x}\|_{\psi_2} < \infty$ and we can indeed find an $\alpha_1 > 0$ to satisfy the inequality. Now suppose that for dimension $d - 1$ there exists an α_{d-1} such that

$$\mathbb{E}_\pi \left[\prod_{i=1}^{d-1} \exp (2\alpha_{d-1} |\mathbf{e}_i^T \mathbf{x}|^2) \right] = C_{d-1} < \infty .$$

By using the Cauchy-Schwarz inequality, we get that

$$\mathbb{E}_\pi \left[\prod_{i=1}^d \exp (2\alpha_d |\mathbf{e}_i^T \mathbf{x}|^2) \right] \leq \mathbb{E}_\pi \left[\prod_{i=1}^{d-1} \exp (4\alpha_d |\mathbf{e}_i^T \mathbf{x}|^2) \right]^{1/2} \mathbb{E}_\pi [\exp (4\alpha_d |\mathbf{e}_d^T \mathbf{x}|^2)]^{1/2} .$$

Taking $\alpha_d \leq \alpha_{d-1}/2$ gives

$$\mathbb{E}_\pi \left[\prod_{i=1}^{d-1} \exp (4\alpha_d |\mathbf{e}_i^T \mathbf{x}|^2) \right]^{1/2} \leq \mathbb{E}_\pi \left[\prod_{i=1}^{d-1} \exp (2\alpha_{d-1} |\mathbf{e}_i^T \mathbf{x}|^2) \right]^{1/2} = C_{d-1}^{1/2} .$$

Taking α_d such that $\frac{1}{\sqrt{4\alpha_d}} > \|\mathbf{x}\|_{\psi_2}$ gives

$$\mathbb{E}_\pi \left[\exp(4\alpha_d |\mathbf{e}_d^T \mathbf{x}|^2) \right]^{1/2} \leq \mathbb{E}_\pi \left[\exp \left(\frac{|\mathbf{e}_d^T \mathbf{x}|^2}{(1/\sqrt{4\alpha_d})^2} \right) \right]^{1/2} \leq \sqrt{2}.$$

Thus, take $\alpha_d < \frac{1}{4} \min\{2\alpha_{d-1}, \|\mathbf{x}\|_{\psi_2}^{-2}\}$, so that

$$\mathbb{E}_\pi \left[\prod_{i=1}^d \exp(2\alpha_d |\mathbf{e}_i^T \mathbf{x}|^2) \right] \leq \sqrt{2C_{d-1}} < \infty.$$

Since the dimension is finite, we know that we will always be able to take $\alpha_d > 0$. Setting $\alpha = \alpha_d$, shows the first direction of the lemma.

For the converse suppose that there exists a symmetric positive-definite matrix $\mathbf{A} \succ 0$ so that for all vectors $\boldsymbol{\mu}$

$$\mathbb{E}_\pi \left[\exp((\mathbf{x} - \boldsymbol{\mu})^T \mathbf{A} (\mathbf{x} - \boldsymbol{\mu})) \right] < \infty.$$

In particular, for $\boldsymbol{\mu} = 0$

$$\mathbb{E}_\pi \left[\exp(\mathbf{x}^T \mathbf{A} \mathbf{x}) \right] = C < \infty.$$

For any $\mathbf{v} \in S^{d-1}$, we have that

$$\mathbb{E}_\pi \left[\exp \left(\frac{|\mathbf{v}^T \mathbf{x}|^2}{t^2} \right) \right] \leq \mathbb{E}_\pi \left[\exp \left(\frac{\|\mathbf{x}\|^2}{t^2} \right) \right],$$

since $|\mathbf{v}^T \mathbf{x}| \leq \|\mathbf{v}\| \|\mathbf{x}\|$. Also, since the minimum eigenvalue satisfies $\lambda_{\min}^{\mathbf{A}} \leq \frac{\mathbf{x}^T \mathbf{A} \mathbf{x}}{\|\mathbf{x}\|^2}$, we get

$$\mathbb{E}_\pi \left[\exp \left(\frac{\|\mathbf{x}\|^2}{t^2} \right) \right] \leq \mathbb{E}_\pi \left[\exp \left(\frac{\mathbf{x}^T \mathbf{A} \mathbf{x}}{\lambda_{\min}^{\mathbf{A}} t^2} \right) \right] = \mathbb{E}_\pi \left[\left\{ \exp(\mathbf{x}^T \mathbf{A} \mathbf{x}) \right\}^{1/\lambda_{\min}^{\mathbf{A}} t^2} \right].$$

If $\lambda_{\min}^{\mathbf{A}} t^2 > 1$, then the function

$$g(x) = x^{1/(\lambda_{\min}^{\mathbf{A}} t^2)}$$

is concave and increasing in x . By Jensen's inequality, we obtain

$$\mathbb{E}_\pi \left[\left\{ \exp(\mathbf{x}^T \mathbf{A} \mathbf{x}) \right\}^{1/\lambda_{\min}^{\mathbf{A}} t^2} \right] \leq \mathbb{E}_\pi \left[\exp(\mathbf{x}^T \mathbf{A} \mathbf{x}) \right]^{1/\lambda_{\min}^{\mathbf{A}} t^2} = C^{1/\lambda_{\min}^{\mathbf{A}} t^2}.$$

Setting $C^{1/\lambda_{\min}^{\mathbf{A}} t^2} \leq 2$ and solving for t gives

$$t \geq \sqrt{\frac{\log C}{\lambda_{\min}^{\mathbf{A}} \log 2}}.$$

Since this inequality holds for every $\mathbf{v} \in S^{d-1}$ we know that $\|\mathbf{x}\|_{\psi_2} < \infty$ and hence \mathbf{x} is sub-Gaussian. \square

In the case where π is a Gaussian with covariance $\boldsymbol{\Sigma}$, the matrix \mathbf{A} must be such that $\frac{1}{2}\boldsymbol{\Sigma}^{-1} - \mathbf{A}$ is symmetric positive definite. Recall that the Orlicz norm determines the tail decay of the distribution. If $\|\mathbf{x}\|_{\psi_2}$ is small then α can be taken to be large since the tails decay quickly. The proof also shows that if $\lambda_{\min}^{\mathbf{A}}$ is small then $\|\mathbf{x}\|_{\psi_2}$ will be large, corresponding to large variance.

3.2 Bounding the χ^2 divergence

In this section we derive the dependence of the MSE of the estimator (6) with respect to $\mathbb{E}_p[f]$ on the fidelity h used to find the biasing density q_h . We bound $\chi^2(p \parallel q_h)$ with respect to h and we want this bound to factor into a part depending only on the ratio p/p_h and a part depending only on the ratio p_h/q_h . The following example demonstrates that such a decomposition is not straightforward: let

$$p = ae^{-ax}, \quad p_h = be^{-bx}, \quad q_h = ce^{-cx}$$

for $a, b, c > 0$, be three exponential distributions. Then

$$\chi^2(p \parallel p_h) = \int_0^\infty \frac{a^2}{b} e^{-(2a-b)x} dx = \frac{a^2}{b(2a-b)}$$

if $a > b/2$ and ∞ otherwise. By taking $a = 2$, $b = 3/2$ and $c = 1$, we have that

$$\chi^2(p \parallel p_h) < \infty, \quad \chi^2(p_h \parallel q_h) < \infty,$$

but that

$$\chi^2(p \parallel q_h) = \infty,$$

which means that we cannot directly decompose the χ^2 divergence into the product of χ^2 divergences with an intermediate distribution. In contrast, the Cauchy-Schwarz inequality gives

$$\chi^2(p \parallel q_h) + 1 = \left\| \frac{p}{q_h} \right\|_{L^1(p)} = \left\langle \frac{p}{p_h}, \frac{p_h}{q_h} \right\rangle_{L^2(p)} \leq \left\| \frac{p}{p_h} \right\|_{L^2(p)} \left\| \frac{p_h}{q_h} \right\|_{L^2(p)}, \quad (7)$$

which requires the likelihood ratios p/p_h and p_h/q_h to be in $L^2(p)$ as opposed to $L^1(p)$ which is required for the bound (3) to hold. The space L^2 is defined as

$$L^2(p) = \left\{ g : \Theta \rightarrow \mathbb{R} \text{ measurable} \mid \int_{\Theta} g(\boldsymbol{\theta})^2 p(\boldsymbol{\theta}) d\boldsymbol{\theta} < \infty \right\},$$

and $L^2(q_h)$ is defined similarly. The next four assumptions are sufficient for the likelihood ratios p/p_h and p_h/q_h to be in $L^2(p)$ and to decompose the χ^2 divergence as in the right-hand-side of Equation (7).

Assumption 1. *The densities p, p_h, q_h have the form*

$$p(\boldsymbol{\theta}) = \frac{1}{Z} e^{-\Phi(\boldsymbol{\theta})}, \quad p_h(\boldsymbol{\theta}) = \frac{1}{Z_h} e^{-\Phi_h(\boldsymbol{\theta})}, \quad q_h(\boldsymbol{\theta}) = \frac{1}{\tilde{Z}_h} e^{-\tilde{\Phi}_h(\boldsymbol{\theta})},$$

with potentials $\Phi, \Phi_h, \tilde{\Phi}_h$, respectively and $\Phi_h(\boldsymbol{\theta}) \rightarrow \Phi(\boldsymbol{\theta})$ for all $\boldsymbol{\theta} \in \Theta$.

Assumption 2. *The density p is sub-Gaussian with matrix \mathbf{A} given by Lemma 1.*

Assumption 3. *There exists $\delta_1(h) > 0$ and a function $c_1(\boldsymbol{\theta}) \geq 0$, such that*

$$\Phi_h(\boldsymbol{\theta}) \leq \Phi(\boldsymbol{\theta}) + \delta_1(h) c_1(\boldsymbol{\theta})$$

for all $\boldsymbol{\theta} \in \Theta$, where $\delta_1(h) \downarrow 0$ as $h \downarrow 0$.

Assumption 4. *There exist $\delta_2(h) > 0$ and a function $c_2(\boldsymbol{\theta}) \geq 0$ such that for all h*

$$\tilde{\Phi}_h(\boldsymbol{\theta}) \leq \Phi_h(\boldsymbol{\theta}) + \delta_2(h) c_2(\boldsymbol{\theta})$$

for all $\boldsymbol{\theta} \in \Theta$.

Note that for Assumption 4 we do not assume that $\delta_2(h) \rightarrow 0$ as $h \rightarrow 0$, because, in Section 3.3, the density q_h will be the Laplace approximation of p_h which does not necessarily converge to p_h as $h \rightarrow 0$, unless p_h itself is a Gaussian. Theorem 1 gives the decomposition and bound depending on the fidelity h .

Theorem 1. *Let Assumptions 1, 2, 3, and 4 hold and assume there exist constants $\delta_1^0, \delta_2^0 > 0$ such that*

$$c_i(\boldsymbol{\theta}) \leq \|\boldsymbol{\theta}\|^2 + \delta_i^0, \quad i = 1, 2.$$

If there exists h_{\max} such that for all $h \leq h_{\max}$

$$2\delta_1(h) \leq \frac{1}{2}\lambda_{\min}^{\mathbf{A}}$$

and

$$2\delta_2(h) \leq \frac{1}{2}\lambda_{\min}^{\mathbf{A}}$$

hold, then for all $h \leq h_{\max}$ we have that

$$\chi^2(p \parallel q_h) + 1 \leq K_0 e^{K_1 \delta_1(h) + K_2 \delta_2(h)} \quad (8)$$

where K_0, K_1, K_2 are all constants independent of h .

Proof. By Assumption 2, p is sub-Gaussian with matrix $\mathbf{A} \succ 0$ so that by Lemma 1

$$\frac{1}{Z} \int_{\Theta} \exp(\boldsymbol{\theta}^T \mathbf{A} \boldsymbol{\theta} - \Phi(\boldsymbol{\theta})) \, d\boldsymbol{\theta} < \infty.$$

Recall that Z is the normalizing constant from Assumption 1.

Part 1: Bounding surrogate to high-fidelity norm

The first term on the right-hand-side of Equation (7) can be bounded using Assumption 3:

$$\begin{aligned} \left\| \frac{p}{p_h} \right\|_{L^2(p)}^2 &= \frac{1}{Z} \left(\frac{Z_h}{Z} \right)^2 \int_{\Theta} \exp \{ 2(\Phi_h(\boldsymbol{\theta}) - \Phi(\boldsymbol{\theta})) - \Phi(\boldsymbol{\theta}) \} \, d\boldsymbol{\theta} \\ &\leq \frac{1}{Z} \left(\frac{Z_h}{Z} \right)^2 \int_{\Theta} \exp \{ 2\delta_1(h) (\|\boldsymbol{\theta}\|^2 + \delta_1^0) - \Phi(\boldsymbol{\theta}) \} \, d\boldsymbol{\theta}. \end{aligned}$$

Re-writing this last line gives

$$\left\| \frac{p}{p_h} \right\|_{L^2(p)}^2 \leq \frac{1}{Z} \left(\frac{Z_h}{Z} \right)^2 \exp(2\delta_1^0 \delta_1(h)) \int_{\Theta} \exp \{ 2\delta_1(h) \|\boldsymbol{\theta}\|^2 - \Phi(\boldsymbol{\theta}) \} \, d\boldsymbol{\theta}. \quad (9)$$

Now the two dependencies of the right-hand-side of (9) on the fidelity h are through the ratio Z_h/Z and through $\delta_1(h)$. For now we just bound the integral on the right-hand-side of (9), which is finite since $\mathbf{A} \succ 2\delta_1(h)\mathbf{I}$ and $h \leq h_{\max}$. Adding and subtracting $\boldsymbol{\theta}^T \mathbf{A} \boldsymbol{\theta}$ in (9) gives

$$\begin{aligned} \left\| \frac{p}{p_h} \right\|_{L^2(p)}^2 &\leq \frac{1}{Z} \left(\frac{Z_h}{Z} \right)^2 \exp(2\delta_1^0 \delta_1(h)) \int_{\Theta} \exp \{ 2\delta_1(h) \|\boldsymbol{\theta}\|^2 - \Phi(\boldsymbol{\theta}) \} \, d\boldsymbol{\theta} \\ &= \frac{1}{Z} \left(\frac{Z_h}{Z} \right)^2 \exp(2\delta_1^0 \delta_1(h)) \int_{\Theta} \exp \{ -\boldsymbol{\theta}^T (\mathbf{A} - 2\delta_1(h)\mathbf{I}) \boldsymbol{\theta} + \boldsymbol{\theta}^T \mathbf{A} \boldsymbol{\theta} - \Phi(\boldsymbol{\theta}) \} \, d\boldsymbol{\theta}. \end{aligned}$$

Putting this together with the fact that $\mathbf{A} - 2\delta_1(h)\mathbf{I} \succ 0$ gives

$$\left\| \frac{p}{p_h} \right\|_{L^2(p)}^2 \leq \frac{1}{Z} \left(\frac{Z_h}{Z} \right)^2 \exp(2\delta_1^0 \delta_1(h)) \int_{\Theta} \exp \{ \boldsymbol{\theta}^T \mathbf{A} \boldsymbol{\theta} - \Phi(\boldsymbol{\theta}) \} \, d\boldsymbol{\theta} \quad (10)$$

to complete the bound of the first term on the right-hand-side of Equation (7).

Part 2: Bounding approximation to surrogate

The second term on the right-hand-side of Equation (7) is bounded in a similar fashion. By Assumption 4 we can bound

$$\begin{aligned} \left\| \frac{p_h}{q_h} \right\|_{L^2(p)}^2 &= \frac{1}{Z} \left(\frac{\tilde{Z}_h}{Z_h} \right)^2 \int_{\Theta} \exp \left\{ 2 \left(\tilde{\Phi}_h(\boldsymbol{\theta}) - \Phi_h(\boldsymbol{\theta}) \right) - \Phi(\boldsymbol{\theta}) \right\} d\boldsymbol{\theta} \\ &\leq \frac{1}{Z} \left(\frac{\tilde{Z}_h}{Z_h} \right)^2 \int_{\Theta} \exp \left\{ 2\delta_2(h) (\|\boldsymbol{\theta}\|^2 + \delta_2^0) - \Phi(\boldsymbol{\theta}) \right\} d\boldsymbol{\theta} \\ &= \frac{1}{Z} \left(\frac{\tilde{Z}_h}{Z_h} \right)^2 \exp(2\delta_2^0\delta_2(h)) \int_{\Theta} \exp \left\{ 2\delta_2(h)\|\boldsymbol{\theta}\|^2 - \Phi(\boldsymbol{\theta}) \right\} d\boldsymbol{\theta}. \end{aligned}$$

Again we add and subtract $\boldsymbol{\theta}^T \mathbf{A} \boldsymbol{\theta}$ to obtain

$$\left\| \frac{p_h}{q_h} \right\|_{L^2(p)}^2 \leq \frac{1}{Z} \left(\frac{\tilde{Z}_h}{Z_h} \right)^2 \exp(2\delta_2^0\delta_2(h)) \int_{\Theta} \exp \left\{ -\boldsymbol{\theta}^T (\mathbf{A} - 2\delta_2(h)\mathbf{I}) \boldsymbol{\theta} + \boldsymbol{\theta}^T \mathbf{A} \boldsymbol{\theta} - \Phi(\boldsymbol{\theta}) \right\} d\boldsymbol{\theta}.$$

Using this with the fact that $\mathbf{A} - 2\delta_2(h)\mathbf{I} \succ 0$ gives

$$\left\| \frac{p_h}{q_h} \right\|_{L^2(p)}^2 \leq \frac{1}{Z} \left(\frac{\tilde{Z}_h}{Z_h} \right)^2 \exp(2\delta_2^0\delta_2(h)) \int_{\Theta} \exp \left\{ \boldsymbol{\theta}^T \mathbf{A} \boldsymbol{\theta} - \Phi(\boldsymbol{\theta}) \right\} d\boldsymbol{\theta}. \quad (11)$$

Multiplying the right-hand-sides of the bounds (10) and (11) and then taking the square root gives

$$\left\| \frac{p}{q_h} \right\|_{L^1(p)} \leq \frac{1}{Z} \left(\frac{\tilde{Z}_h}{Z_h} \right) \exp \left\{ \delta_1(h)\delta_1^0 + \delta_2(h)\delta_2^0 \right\} \int_{\Theta} \exp \left\{ \boldsymbol{\theta}^T \mathbf{A} \boldsymbol{\theta} - \Phi(\boldsymbol{\theta}) \right\} d\boldsymbol{\theta}. \quad (12)$$

The integral is independent of h , so it remains to bound the ratio of normalizing constants.

Part 3: Bounding ratio of normalizing constants

In general, if p_h is not in the family of approximations then we may have $\tilde{Z}_h \neq Z_h$, and thus,

$$\frac{\tilde{Z}_h}{Z_h} \not\rightarrow 1$$

as $h \rightarrow 0$. Instead we just give a constant upper bound on \tilde{Z}_h that is independent of the fidelity h . By Assumption 1, the normalizing constant \tilde{Z}_h satisfies

$$\begin{aligned} \tilde{Z}_h &= \int_{\Theta} e^{-\tilde{\Phi}_h(\boldsymbol{\theta})} d\boldsymbol{\theta} \\ &= \int_{\Theta} \exp \left\{ -\tilde{\Phi}_h(\boldsymbol{\theta}) + \Phi_h(\boldsymbol{\theta}) - \Phi_h(\boldsymbol{\theta}) + \Phi(\boldsymbol{\theta}) - \Phi(\boldsymbol{\theta}) \right\} d\boldsymbol{\theta} \\ &= Z \int_{\Theta} \exp \left\{ -\tilde{\Phi}_h(\boldsymbol{\theta}) + \Phi_h(\boldsymbol{\theta}) - \Phi_h(\boldsymbol{\theta}) + \Phi(\boldsymbol{\theta}) \right\} p(\boldsymbol{\theta}) d\boldsymbol{\theta}. \end{aligned}$$

Dividing by Z and using Assumptions 3 and 4 we have

$$\frac{\tilde{Z}_h}{Z} \leq \int_{\Theta} \exp \left\{ -\delta_1(h)(\|\boldsymbol{\theta}\|^2 + \delta_1^0) - \delta_2(h)(\|\boldsymbol{\theta}\|^2 + \delta_2^0) \right\} p(\boldsymbol{\theta}) d\boldsymbol{\theta} \leq 1. \quad (13)$$

Finally, combining the bounds (10), (11), and (13) gives the result

$$\chi^2(p \parallel q_h) + 1 = \left\| \frac{p}{q_h} \right\|_{L^1(p)} \leq \exp \{ \delta_1(h) \delta_1^0 + \delta_2(h) \delta_2^0 \} \mathbb{E}_p [\exp(\boldsymbol{\theta}^T \mathbf{A} \boldsymbol{\theta})],$$

where the expectation is independent of h . Here

$$K_0 = \mathbb{E}_p [\exp(\boldsymbol{\theta}^T \mathbf{A} \boldsymbol{\theta})], \quad K_1 = \delta_1^0, \quad \delta_2^0 = K_2$$

are all independent of the fidelity h . □

Remark 1. *The assumption that $c_i(\boldsymbol{\theta}) \leq \|\boldsymbol{\theta}\|^2 + \delta_i^0$ for $i = 1, 2$ holds is similar to the pointwise Assumption 4.8 in Theorem 4.6 of [35]. In [35], the pointwise bound can be larger than in our case because the Hellinger distance is considered in [35].*

3.3 Laplace approximation

In this section, we consider the Laplace approximation of a density as a specific choice of biasing density q_h . The Laplace approximation is a Gaussian approximation defined as follows.

Definition 1. *The Laplace approximation to a distribution p_h is the Gaussian distribution whose mean is*

$$\boldsymbol{\mu}_h^{\text{LAP}} = \underset{\boldsymbol{\theta} \in \Theta}{\operatorname{argmin}} -\log p_h(\boldsymbol{\theta}) = \underset{\boldsymbol{\theta} \in \Theta}{\operatorname{argmin}} \Phi_h(\boldsymbol{\theta}),$$

and whose covariance is the negative inverse Hessian of the log-likelihood evaluated at the mode

$$\boldsymbol{\Sigma}_h^{\text{LAP}} = -[\nabla \nabla^T \log p_h(\boldsymbol{\mu}_h^{\text{LAP}})]^{-1} = [\nabla \nabla^T \Phi_h(\boldsymbol{\mu}_h^{\text{LAP}})]^{-1}.$$

Additionally we need the following assumption that the covariance of the Laplace approximations does not collapse to a hyper-plane.

Assumption 5. *Assume there exists a $\sigma_{\min}^2 > 0$ such that*

$$\boldsymbol{\theta}^T \boldsymbol{\Sigma}_h^{\text{LAP}} \boldsymbol{\theta} \geq \sigma_{\min}^2 \|\boldsymbol{\theta}\|^2$$

for all $\boldsymbol{\theta} \in \Theta$ and h .

It follows from Assumption 5 that

$$\boldsymbol{\theta}^T (\boldsymbol{\Sigma}_h^{\text{LAP}})^{-1} \boldsymbol{\theta} \leq \frac{1}{\sigma_{\min}^2} \|\boldsymbol{\theta}\|^2. \tag{14}$$

for all $\boldsymbol{\theta} \in \Theta$ and h . Assumption 5 is the same as Equation (34) from Proposition 2 in [34], although in our case the inequality needs to hold uniformly for all h . Proposition 1 gives conditions for the Laplace approximation to be a suitable biasing density.

Proposition 1. *If Assumption 5 holds and there exist constants $M, \epsilon > 0$ such that*

$$\Phi_h(\boldsymbol{\theta}) > M - \epsilon \|\boldsymbol{\theta}\|^2 \tag{15}$$

for all h , then the Laplace approximation satisfies Assumption 4.

Proof. The Laplace approximation is a second-order Taylor expansion around the mode

$$\Phi_h(\boldsymbol{\theta}) = \Phi_h(\boldsymbol{\mu}_h^{\text{LAP}}) + \frac{1}{2} (\boldsymbol{\theta} - \boldsymbol{\mu}_h^{\text{LAP}})^T [\nabla \nabla^T \Phi_h(\boldsymbol{\mu}_h^{\text{LAP}})] (\boldsymbol{\theta} - \boldsymbol{\mu}_h^{\text{LAP}}) + R_h(\boldsymbol{\theta}).$$

The first derivative is zero since it is expanded around the minimizer and $R_h(\boldsymbol{\theta})$ is the remainder. Therefore,

$$\tilde{\Phi}_h(\boldsymbol{\theta}) - \Phi_h(\boldsymbol{\theta}) = -R_h(\boldsymbol{\theta}).$$

Using the bounds (15) and (14) gives

$$\begin{aligned} \tilde{\Phi}_h(\boldsymbol{\theta}) - \Phi_h(\boldsymbol{\theta}) &\leq \tilde{\Phi}_h(\boldsymbol{\theta}) - M + \epsilon \|\boldsymbol{\theta}\|^2 \\ &\leq \Phi_h(\boldsymbol{\mu}_h^{\text{LAP}}) + \frac{1}{2\sigma_{\min}^2} \|\boldsymbol{\theta} - \boldsymbol{\mu}_h^{\text{LAP}}\|^2 - M + \epsilon \|\boldsymbol{\theta}\|^2. \end{aligned}$$

Combining this with the fact that $\|\mathbf{x} + \mathbf{y}\|^2 \leq 2\|\mathbf{x}\|^2 + 2\|\mathbf{y}\|^2$ yields

$$\tilde{\Phi}_h(\boldsymbol{\theta}) - \Phi_h(\boldsymbol{\theta}) \leq \Phi_h(\boldsymbol{\mu}_h^{\text{LAP}}) + \left(\frac{1}{\sigma_{\min}} + \epsilon \right) \|\boldsymbol{\theta}\|^2 + \frac{1}{\sigma_{\min}^2} \|\boldsymbol{\mu}_h^{\text{LAP}}\|^2 - M.$$

Since $\Phi_h(\boldsymbol{\theta}) \rightarrow \Phi(\boldsymbol{\theta})$ for each $\boldsymbol{\theta} \in \Theta$ as $h \rightarrow 0$ we know that $\Phi_h(\boldsymbol{\mu}_h^{\text{LAP}})$ and $\|\boldsymbol{\mu}_h^{\text{LAP}}\|^2$ can be bounded by constants independent of h (since they both converge). \square

The additional assumption in Equation (15) in Proposition 1 is exactly Assumption 2.6 (i) from [35] and a pointwise bound is needed to match Assumption 4 from earlier that $c_2(\boldsymbol{\theta}) \leq \|\boldsymbol{\theta}\|^2 + \delta_2^0$. This pointwise assumption is needed to prevent pathological cases such as the following example of a sub-Gaussian distribution that violates the pointwise requirement. Let $p(x) \propto \exp(-\Phi(x))$ with

$$\Phi(x) = \begin{cases} -n^4, & x \in [n, n + \exp(-n^4 - (n+1)^2)n^{-2}] \quad \forall n \in \mathbb{N} \\ 2x^2, & \text{otherwise} \end{cases}$$

then,

$$\int_{\mathbb{R}} e^{x^2} p(x) dx < \int_{\mathbb{R}} e^{-x^2} dx + \sum_{n=1}^{\infty} e^{(n+1)^2} e^{n^4} \times e^{-n^4 - (n+1)^2} n^{-2} < \infty,$$

showing that the density can oscillate between very large negative values and positive values while still being integrable.

3.4 Optimal trade-off for finding context-aware surrogate-model fidelity

We now define the optimal trade-off and derive the fidelity of context-aware surrogate models.

3.4.1 Optimal trade-off

The total computational cost of estimating $\mathbb{E}_p[f]$ with the MFIS estimator (6) can be decomposed into an offline training cost to fit the biasing density q_h as well as an online cost to sample and re-weight; cf. Section 3.5. Recall that C_{hi} denotes the cost of a single evaluation of the un-normalized high-fidelity density \tilde{p} and that $c^{\text{train}}(h)$ is the total offline training cost when using the surrogate density p_h . This training cost includes both the cost required to construct the un-normalized density \tilde{p}_h as well as to fit the biasing density q_h . In contrast, the online cost to draw m samples and re-weight them with the high-fidelity density is

$$c^{\text{online}}(h) = mC_{\text{hi}}.$$

Note that the online cost depends implicitly on the fidelity h since the number of samples that are needed is determined by $\chi^2(p \parallel q_h)$, which we have just bounded previously. If the number of samples m is fixed, then this cost is independent of the the fidelity since the samples are drawn from a Gaussian distribution (Laplace approximation) with costs independent of h . We make one assumption on the form of the MSE.

Assumption 6. *The MSE can be bounded as*

$$\mathbb{E} \left[\left(\hat{f}_{h,m} - \mathbb{E}_p[f] \right)^2 \right] \leq \frac{1}{m} \text{err}(h),$$

where $\text{err}(h) \geq 0$ for all h and $\text{err} \rightarrow 0$ as $h \rightarrow 0$.

Note that this form exactly matches what we derived in Theorem 1. However, the result that follows does not assume that the biasing density is necessarily the Laplace approximation to the surrogate density. The optimization problem to minimize total computational cost with a fixed error tolerance is

$$\begin{aligned} & \underset{m, h \geq 0}{\text{minimize}} && mC_{\text{hi}} + c^{\text{train}}(h) \\ & \text{subject to} && \frac{1}{m} \text{err}(h) \leq \epsilon. \end{aligned} \tag{16}$$

Theorem 2. *Suppose that $c^{\text{train}}, \text{err}$ are non-negative convex functions, not necessarily strictly convex, and that c^{train} increases monotonically and err decreases monotonically as $h \rightarrow 0$. Then there exists a unique solution (h^*, m^*) to the minimization problem (16).*

Proof. For any h , the optimal m is the one that achieves equality in the constraint

$$m = \frac{1}{\epsilon} \text{err}(h).$$

Plugging this into the objective function gives the minimization problem over h only.

$$\underset{h \geq 0}{\text{minimize}} \quad \frac{C_{\text{hi}}}{\epsilon} \text{err}(h) + c^{\text{train}}(h). \tag{17}$$

Since the sum of convex functions is convex, we know that this new objective function in h is convex. Hence, if a minimum exists it is unique.

We next claim that the optimal value of (17) is not attained at $h = \infty$. In other words, there exists $h_{\text{max}} \in (0, \infty)$ so that $h^* \leq h_{\text{max}}$. Since c^{train} is monotonically decreasing and convex as $h \rightarrow \infty$, we must have that $c^{\text{train}}(h) \downarrow c_0 \geq 0$ is bounded below by some c_0 as $h \rightarrow \infty$. However, $\text{err}(h) \rightarrow \infty$ as $h \rightarrow \infty$ and so the objective function is unbounded in h as $h \rightarrow \infty$ and increasing for h sufficiently large. Thus, we may only consider the minimization over the interval $[0, h_{\text{max}}]$. Since the objective is continuous over a compact set we know that a minimizer h^* exists. \square

Assuming that both c^{train} and err are differentiable and using the notation $'$ to denote the derivative with respect to h , the optimal solution satisfies

$$\frac{C_{\text{hi}}}{\epsilon} \text{err}'(h^*) + (c^{\text{train}})'(h^*) = 0,$$

so that isolating ϵ gives

$$-C_{\text{hi}} \frac{\text{err}'(h^*)}{(c^{\text{train}})'(h^*)} = \epsilon.$$

As $\epsilon \rightarrow 0$ we must have $\frac{\text{err}'(h^*)}{(c^{\text{train}})'(h^*)} \rightarrow 0$. If the optimal fidelity h^* is to remain bounded above zero in the limit as $\epsilon \rightarrow 0$, then we must have either $\text{err}'(h)$ is zero at some $h > 0$ or $(c^{\text{train}})'(h) = \infty$ at some $h > 0$ (i.e., unbounded at some positive finite fidelity). In the context of our problem, in order for err' to be zero we would need the surrogate density p_h to exactly be the high-fidelity density.

3.4.2 Optimal trade-off when Laplace approximation is biasing density

In fitting the

Laplace approximation we assume that a fixed number of evaluations M_{fit} are needed to fit the biasing density and that this number is independent of the fidelity h . For example, M_{fit} could be the total number of model evaluations used in Newton's method until machine precision is reached where both the gradient and Hessian are computed using finite differences as well as computing the Hessian at the mode. As a result, the total offline training cost to fit the biasing density is

$$c^{\text{train}}(h) = M_{\text{fit}}c(h),$$

where $c(h)$ is the cost of evaluating the un-normalized surrogate density \tilde{p}_h . Moreover, by Equation (8) and Theorem (3), we know that Assumption 6 is satisfied with

$$\text{err}(h) = 4\|f\|_{L^\infty}K_0e^{K_1\delta(h)}$$

for some non-negative constants K_0, K_1 and a decreasing function δ , that is convex in h . Note that this K_0 is slightly different from the K_0 in Equation (8), but is still independent of h .

Corollary 1. *Let c be a non-negative decreasing convex function with h and let δ be a non-negative increasing convex function of h . Then the following optimization problem for the optimal fidelity and number of samples has a unique solution.*

$$\begin{aligned} & \underset{m, h \geq 0}{\text{minimize}} && mC_{\text{hi}} + M_{\text{fit}}c(h) \\ & \text{subject to} && \frac{4\|f\|_{L^\infty}K_0}{m} \exp(K_1\delta(h)) \leq \epsilon \end{aligned} \quad (18)$$

Proof. Because the composition of convex functions is still convex, we know that err must be convex and therefore satisfies the assumptions of Theorem 2. \square

As in the proof of Theorem 2, we can remove the constraint to instead minimize

$$\underset{h \geq 0}{\text{minimize}} \quad \frac{4\|f\|_{L^\infty}K_0C_{\text{hi}}}{\epsilon} \exp(K_1\delta(h)) + M_{\text{fit}}c(h), \quad (19)$$

which is analogous to (17). The next two examples are special cases of (18) with $c(h)$ and $\delta(h)$ specified.

Example 1. Consider $c(h) = \beta^{1/h}$ and $\delta(h) = \alpha^{-1/h}$ with $\alpha, \beta > 1$. By setting the derivative of (19) with respect to h to zero, the optimal solution satisfies

$$\log \epsilon = -h^{-1} \log(\alpha\beta) + K_1\alpha^{-1/h} + \log \left(\frac{4\|f\|_{L^\infty}C_{\text{hi}}K_0K_1 \log \alpha}{M_{\text{fit}} \log \beta} \right),$$

meaning that $1/h^* = O(\log \epsilon^{-1})$ as $\epsilon \rightarrow 0$. If we set $1/\tilde{h} = \log_\alpha \epsilon^{-1}$ exactly, then the number of samples needed is

$$\tilde{m} = \frac{4\|f\|_{L^\infty}K_0}{\epsilon} \exp(K_1\epsilon)$$

with a total computational budget

$$\tilde{b} = \frac{4\|f\|_{L^\infty}C_{\text{hi}}K_0}{\epsilon} \exp(K_1\epsilon) + M_{\text{fit}}\beta^{\log_\alpha \epsilon^{-1}}$$

compared to the total computational cost with a fixed fidelity h

$$b(h) = \frac{4\|f\|_{L^\infty}C_{\text{hi}}K_0}{\epsilon} \exp(K_1\alpha^{-1/h}) + M_{\text{fit}}\beta^{1/h}.$$

Example 2. Consider $c(h) = h^{-\beta}$ and $\delta(h) = h^\alpha$ with $\alpha, \beta \geq 1$. Again set the derivative to zero to find that the optimal solution satisfies

$$\frac{4\|f\|_{L^\infty} C_{\text{hi}} K_0 K_1}{M} \left(\frac{\alpha}{\beta} \right) \exp(K_1 h^\alpha) h^{\alpha+\beta} = \epsilon,$$

so that $h^* = O(\epsilon^{1/(\alpha+\beta)})$ as $\epsilon \rightarrow 0$. If we use a variable fidelity $\tilde{h} = \epsilon^{1/(\alpha+\beta)}$, then the number of samples needed is

$$\tilde{m} = \frac{4\|f\|_{L^\infty} K_0}{\epsilon} \exp(K_1 \epsilon^{\alpha/(\alpha+\beta)})$$

with total computational budget

$$\tilde{b} = \frac{4\|f\|_{L^\infty} C_{\text{hi}} K_0}{\epsilon} \exp(K_1 \epsilon^{\alpha/(\alpha+\beta)}) + M_{\text{fit}} \epsilon^{-\beta/(\alpha+\beta)}$$

compared to the total computational cost with a fixed fidelity h

$$b(h) = \frac{4\|f\|_{L^\infty} C_{\text{hi}} K_0}{\epsilon} \exp(K_1 h^\alpha) + M_{\text{fit}} h^{-\beta}.$$

3.5 Computational procedure

Algorithm 1 Context-aware importance sampling

- 1: Constants $K_0, K_1, C_{\text{hi}}, \epsilon, M_{\text{fit}}$ and functions c, δ
 - 2: Solve the optimization problem (18) for (h^*, m^*) using $\|f\|_{L^\infty}, K_0, K_1, C_{\text{hi}}, M_{\text{fit}}, \epsilon, c, \delta$
 - 3: Compute the Laplace approximation q_{h^*} of p_{h^*} with M_{fit} evaluations of p_{h^*}
 - 4: Draw m^* i.i.d. samples $\{\theta^{(i)}\}_{i=1}^{m^*}$ from q_{h^*}
 - 5: Compute \hat{f}_{h^*, m^*} using (6) **return** Estimate \hat{f}_{h^*, m^*}
-

Algorithm 1 summarizes the context-aware importance sampling procedure. Given constants $K_0, K_1, C_{\text{hi}}, M_{\text{fit}}$, and the tolerance ϵ as well as the cost and accuracy functions c and δ , the context-aware importance sampling Algorithm 1 first solves the optimization problem 18 for (h^*, m^*) . The Laplace approximation to the surrogate density p_{h^*} is then computed using Newton's method. In particular, we use the Newton-CG method where both the gradient and Hessian are computed using finite differences. The Hessian at the mode is then inverted directly to obtain the covariance of the Laplace approximation. This concludes the offline phase of finding the biasing density. For the online phase we draw m^* samples from the Laplace approximation q_{h^*} and re-weight using the un-normalized high-fidelity density \tilde{p} using the estimator (6).

4 Bayesian inverse problems

We now apply our results to inference in Bayesian inverse problems where p is a posterior distribution and we are interested in expectations $\mathbb{E}_p[f]$ of this distribution. Section 4.1 describes the general setup of a Bayesian inverse problem and Section 4.2 is the application of our results.

4.1 Setup of a Bayesian inverse problem

We assume we are given data $\mathbf{y} \in \mathbb{R}^{d'}$ generated by an unknown parameter $\theta_{\text{truth}} \in \mathbb{R}^d$ with a Gaussian noise model,

$$\mathbf{y} = \mathcal{F}(\theta_{\text{truth}}) + \eta,$$

where $\boldsymbol{\eta} \sim N(0, \boldsymbol{\Gamma})$, $\boldsymbol{\Gamma} \in \mathbb{R}^{d' \times d'}$ is the covariance matrix (symmetric and positive definite) of the added noise, and $\mathcal{F} : \Theta \rightarrow \mathbb{R}^{d'}$ is the high-fidelity parameter-to-observable map. Let π_{pr} denote a prior distribution over the parameter $\boldsymbol{\theta}$, so that the negative log-posterior has the form

$$-\log p(\boldsymbol{\theta}) = \Phi(\boldsymbol{\theta}) = \frac{1}{2} \|\mathbf{y} - \mathcal{F}(\boldsymbol{\theta})\|_{\boldsymbol{\Gamma}^{-1}}^2 - \log \pi_{\text{pr}}(\boldsymbol{\theta}).$$

The norm is defined by $\|\mathbf{v}\|_{\boldsymbol{\Gamma}^{-1}}^2 = \langle \boldsymbol{\Gamma}^{-1} \mathbf{v}, \mathbf{v} \rangle$. While it is possible to use the prior distribution as a biasing density, if the posterior contracts around the data then the χ^2 divergence from the posterior to the prior may be very large resulting in a high variance estimator with a low effective sample size.

Let \mathcal{F}_h denote the surrogate parameter-to-observable map with fidelity h and be such that the sequence $\mathcal{F}_h(\boldsymbol{\theta}) \rightarrow \mathcal{F}(\boldsymbol{\theta})$ converges pointwise for each $\boldsymbol{\theta} \in \Theta$. In many cases the parameter-to-observable map \mathcal{F} is a function of an intermediate state variable u , such as the full solution to a parametrized partial differential equation (PDE) depending on the parameters $\boldsymbol{\theta}$. The surrogate parameter-to-observable map \mathcal{F}_h is given by approximating this state variable u with an approximation u_h . The approximation for the state variable u_h could be given by finite elements [4], finite difference [21], a different time step for an ordinary differential equation [21], finitely many terms in a Karhunen-Loeve expansion [36], and others.

We consider the case where the prior π_{pr} is Gaussian $N(\boldsymbol{\mu}_{\text{pr}}, \boldsymbol{\Sigma}_{\text{pr}})$, so that we can write the potential from Assumption 1 as

$$\Phi(\boldsymbol{\theta}) = \frac{1}{2} \|\mathbf{y} - \mathcal{F}(\boldsymbol{\theta})\|_{\boldsymbol{\Gamma}^{-1}}^2 + \frac{1}{2} (\boldsymbol{\theta} - \boldsymbol{\mu}_{\text{pr}})^T \boldsymbol{\Sigma}_{\text{pr}}^{-1} (\boldsymbol{\theta} - \boldsymbol{\mu}_{\text{pr}}). \quad (20)$$

With a Gaussian prior the resulting posterior distribution is always sub-Gaussian since we can take the matrix $\mathbf{A} = \frac{1}{4} \boldsymbol{\Sigma}_{\text{pr}}^{-1}$ in Lemma 1. The potentials Φ_h are defined similarly but with the surrogate maps \mathcal{F}_h replacing \mathcal{F} . Here sub-Gaussian is a form of well-posedness with either the prior or likelihood being able to concentrate around the maximum a-posteriori (MAP) point sufficiently and being able to distinguish a unique parameter $\boldsymbol{\theta} \in \Theta$. In other words, we avoid multi-modal posteriors.

4.2 Bounding χ^2 divergence with model error

We now translate bounds on the model error between \mathcal{F} and \mathcal{F}_h to the χ^2 divergence $\chi^2(p \parallel q_h)$, where q_h is still the Laplace approximation to the surrogate posterior p_h . The next two assumptions allow us to make the transition.

Assumption 7. *The high-fidelity parameter-to-observable map \mathcal{F} is globally Lipschitz meaning there exists a constant $B > 0$ such that for all $\boldsymbol{\theta}, \tilde{\boldsymbol{\theta}} \in \Theta$*

$$\|\mathcal{F}(\boldsymbol{\theta}) - \mathcal{F}(\tilde{\boldsymbol{\theta}})\| \leq B \|\boldsymbol{\theta} - \tilde{\boldsymbol{\theta}}\|.$$

Assumption 7 is almost the Lipschitz Assumption 2.7 (ii) from [35] except there the constant B only needs to hold for bounded sets of $\boldsymbol{\theta}$. Assumption 7 is satisfied if the map \mathcal{F} is linear or bounded, for example.

Assumption 8. *For all $\boldsymbol{\theta} \in \Theta$ and h we have*

$$\|\mathcal{F}_h(\boldsymbol{\theta}) - \mathcal{F}(\boldsymbol{\theta})\| \leq \delta(h) c(\boldsymbol{\theta})$$

with $\delta(h) \rightarrow 0$ as $h \rightarrow 0$ with $c(\boldsymbol{\theta})$ independent of h .

Assumption 8 is similar to Assumption (4.11) in Corollary 4.9 of [35], although the pointwise bound is also looser there than here for the same reason as given in Remark 1. Theorem 3 is analogous to Theorem 1 from earlier but now is applied specifically to the Bayesian inverse problem.

Theorem 3. *If Assumptions 7 and 8 are satisfied with $|c(\boldsymbol{\theta})| \leq \|\boldsymbol{\theta}\| + \delta_0$ for some $\delta_0 > 0$, then Assumptions 3, 4 are also satisfied and*

$$\chi^2(p \parallel q_h) + 1 \leq K_0 \exp \{K_1 \delta(h)\} \quad (21)$$

for some constants K_0, K_1 independent of h .

Proof. Using the form of the log-posterior (20) we may write

$$|\Phi_h(\boldsymbol{\theta}) - \Phi(\boldsymbol{\theta})| = \left| \|\mathcal{F}_h(\boldsymbol{\theta}) - \mathbf{y}\|_{\mathbf{\Gamma}^{-1}}^2 - \|\mathcal{F}(\boldsymbol{\theta}) - \mathbf{y}\|_{\mathbf{\Gamma}^{-1}}^2 \right|$$

since the prior terms will cancel. To simplify notation, set $\Delta(\boldsymbol{\theta}) = \mathcal{F}(\boldsymbol{\theta}) - \mathcal{F}_h(\boldsymbol{\theta})$ and $m(\boldsymbol{\theta}) = \mathcal{F}(\boldsymbol{\theta}) - \mathbf{y}$, so that $m(\boldsymbol{\theta}) - \Delta(\boldsymbol{\theta}) = \mathcal{F}_h(\boldsymbol{\theta}) - \mathbf{y}$. Now, we can instead write

$$\begin{aligned} |\Phi_h(\boldsymbol{\theta}) - \Phi(\boldsymbol{\theta})| &= \left| \|m(\boldsymbol{\theta})\|_{\mathbf{\Gamma}^{-1}}^2 - \|m(\boldsymbol{\theta}) - \Delta(\boldsymbol{\theta})\|_{\mathbf{\Gamma}^{-1}}^2 \right| \\ &= \left| \|m(\boldsymbol{\theta})\|_{\mathbf{\Gamma}^{-1}}^2 - \langle \mathbf{\Gamma}^{-1}(m(\boldsymbol{\theta}) - \Delta(\boldsymbol{\theta})), m(\boldsymbol{\theta}) - \Delta(\boldsymbol{\theta}) \rangle \right| \\ &= \left| 2\langle \Delta(\boldsymbol{\theta}), \mathbf{\Gamma}^{-1}m(\boldsymbol{\theta}) \rangle - \|\Delta(\boldsymbol{\theta})\|_{\mathbf{\Gamma}^{-1}}^2 \right|. \end{aligned}$$

Applying the triangle inequality and then the Cauchy-Schwarz inequality to this last line gives

$$|\Phi_h(\boldsymbol{\theta}) - \Phi(\boldsymbol{\theta})| \leq 2\|\Delta(\boldsymbol{\theta})\| \cdot \|\mathbf{\Gamma}^{-1}m(\boldsymbol{\theta})\| + \|\Delta(\boldsymbol{\theta})\|_{\mathbf{\Gamma}^{-1}}^2. \quad (22)$$

Using the fact that $\mathbf{y} = \mathcal{F}(\boldsymbol{\theta}_{\text{truth}}) + \boldsymbol{\eta}$ and the triangle inequality gives

$$\begin{aligned} \|\mathbf{\Gamma}^{-1}m(\boldsymbol{\theta})\| &= \|\mathbf{\Gamma}^{-1}(\mathcal{F}(\boldsymbol{\theta}) - \mathbf{y})\| \\ &\leq \|\mathbf{\Gamma}^{-1}(\mathcal{F}(\boldsymbol{\theta}) - \mathcal{F}(\boldsymbol{\theta}_{\text{truth}}))\| + \|\mathbf{\Gamma}^{-1}\boldsymbol{\eta}\|. \end{aligned}$$

Assumption 7 then gives the bound

$$\|\mathbf{\Gamma}^{-1}m(\boldsymbol{\theta})\| \leq \frac{B}{\gamma_{\min}} \|\boldsymbol{\theta} - \boldsymbol{\theta}_{\text{truth}}\| + \|\mathbf{\Gamma}^{-1}\boldsymbol{\eta}\|, \quad (23)$$

where $\gamma_{\min} > 0$ is the smallest eigenvalue of the covariance matrix $\mathbf{\Gamma}$, i.e. the direction along which the posterior is most peaked. Similarly we may bound

$$\|\Delta(\boldsymbol{\theta})\|_{\mathbf{\Gamma}^{-1}}^2 = \langle \mathbf{\Gamma}^{-1}\Delta(\boldsymbol{\theta}), \Delta(\boldsymbol{\theta}) \rangle \leq \frac{1}{\gamma_{\min}} \|\Delta(\boldsymbol{\theta})\|^2. \quad (24)$$

Substituting the bounds (23) and (24) into (22) yields

$$|\Phi_h(\boldsymbol{\theta}) - \Phi(\boldsymbol{\theta})| \leq 2 \left(\frac{B}{\gamma_{\min}} (\|\boldsymbol{\theta} - \boldsymbol{\theta}_{\text{truth}}\|) + \|\mathbf{\Gamma}^{-1}\boldsymbol{\eta}\| \right) \|\Delta(\boldsymbol{\theta})\| + \frac{1}{\gamma_{\min}} \|\Delta(\boldsymbol{\theta})\|^2,$$

and the triangle inequality gives

$$|\Phi_h(\boldsymbol{\theta}) - \Phi(\boldsymbol{\theta})| \leq 2 \left(\frac{B}{\gamma_{\min}} (\|\boldsymbol{\theta}\| + \|\boldsymbol{\theta}_{\text{truth}}\|) + \|\mathbf{\Gamma}^{-1}\boldsymbol{\eta}\| \right) \|\Delta(\boldsymbol{\theta})\| + \frac{1}{\gamma_{\min}} \|\Delta(\boldsymbol{\theta})\|^2. \quad (25)$$

Note that the term $\|\mathbf{\Gamma}^{-1}\boldsymbol{\eta}\|$ is on the order of γ_{\min}^{-1} as well. Assumption 8 along with the assumption that $|c(\boldsymbol{\theta})| \leq \|\boldsymbol{\theta}\| + \delta_0$ says $\|\Delta(\boldsymbol{\theta})\| \leq \delta(h) (\|\boldsymbol{\theta}\| + \delta_0)$, so we get that

$$|\Phi_h(\boldsymbol{\theta}) - \Phi(\boldsymbol{\theta})| \leq 2 \left(\frac{B}{\gamma_{\min}} (\|\boldsymbol{\theta}\| + \|\boldsymbol{\theta}_{\text{truth}}\|) + \|\mathbf{\Gamma}^{-1}\boldsymbol{\eta}\| \right) \delta(h) (\|\boldsymbol{\theta}\| + \delta_0) + \frac{1}{\gamma_{\min}} \delta(h)^2 (\|\boldsymbol{\theta}\| + \delta_0)^2.$$

Factoring out $\delta(h)$ and using the fact that $\delta(h) \leq \delta(h_{\max})$ for all $h \leq h_{\max}$ gives

$$|\Phi_h(\boldsymbol{\theta}) - \Phi(\boldsymbol{\theta})| \leq \delta(h) \tilde{c}(\boldsymbol{\theta}),$$

where $\tilde{c}(\boldsymbol{\theta})$ is quadratic in $\|\boldsymbol{\theta}\|$ and independent of h . □

5 Numerical Results

This section demonstrates our context-aware importance sampling approach on two examples. All runtime measurements were performed on compute nodes equipped with Intel Xeon Gold 6148 2.4GHz processors and 192GB of memory using a Python 3.6 implementation.

5.1 Steady-state heat conduction

In the first example we consider a steady-state heat diffusion model with constant heat source and infer a 6-dimensional variable diffusivity.

5.1.1 Problem Setup

Let $\Omega = (0, 1) \subset \mathbb{R}$ and $\Theta = \mathbb{R}^6$ and consider the PDE

$$\begin{aligned} -(\exp(k(x; \boldsymbol{\theta})) u_x(x; \boldsymbol{\theta}))_x &= 1, & x \in \Omega \\ u(0; \boldsymbol{\theta}) &= 0 \\ k(1; \boldsymbol{\theta}) u_x(1; \boldsymbol{\theta}) &= 0 \end{aligned} \tag{26}$$

where $\boldsymbol{\theta} = (\theta_1, \dots, \theta_6)^T \in \Theta$, $k : \Omega \times \Theta \rightarrow \mathbb{R}$ is the log-diffusivity, and $u : \Omega \times \Theta \rightarrow \mathbb{R}$ is the temperature function. The log-diffusivity $k(x; \boldsymbol{\theta})$ is a smoothed piecewise constant. In particular, let

$$I(x, \alpha) = \left(1 + \exp\left(-\frac{x - \alpha}{0.005}\right)\right)^{-1}$$

and $\alpha_i = (i - 1)/6$ for $i = 1, \dots, 7$. Define

$$\hat{k}_i(x; \boldsymbol{\theta}) = (1 - I(x, \alpha_i)) \hat{k}_{i-1}(x; \boldsymbol{\theta}) + I(x, \alpha_i) \theta_i \tag{27}$$

for $i = 2, \dots, 6$ and $\hat{k}_1(x; \boldsymbol{\theta}) = \theta_1$. Now set the log-diffusivity $k = \hat{k}_6$. We discretize (26) in the spatial domain Ω using linear finite elements with mesh width $h > 0$ (i.e. h^{-1} many elements) and the corresponding sparse (tri-diagonal) linear system is solved using a Cholesky factorization. The parameter-to-observable map $\mathcal{F}_h : \Theta \rightarrow \mathbb{R}^{120}$ is the discretized solution u_h with mesh width h evaluated at 120 equally-spaced points on Ω

$$(\mathcal{F}_h(\boldsymbol{\theta}))_i = u_h(i/120), \quad i = 1, \dots, 120.$$

For the high-fidelity parameter-to-observable map we set $H^{-1} = 256$ elements, (i.e. $\mathcal{F} = \mathcal{F}_H$) and for the surrogate maps \mathcal{F}_h we consider $h^{-1} = 8, 12, 16, \dots, 64$ (multiples of 4 for the number of elements).

5.1.2 Setup of the inverse problem

A single observation $\mathbf{y} = \mathcal{F}(\boldsymbol{\theta}_{\text{truth}}) + \boldsymbol{\eta}$ is generated where $\boldsymbol{\theta}_{\text{truth}} = (1, \dots, 1)^T \in \mathbb{R}^6$ and $\boldsymbol{\eta} \sim N(\mathbf{0}, 10^{-5} \mathbf{I}_{120 \times 120})$. The added noise corresponds to approximately 1% of the true solution u at the right endpoint $x = 1$. The prior distribution is taken to be a Gaussian with mean $\boldsymbol{\mu}_{\text{pr}} = (1, \dots, 1)^T \in \mathbb{R}^6$ and covariance $\boldsymbol{\Sigma}_{\text{pr}} = 10^{-1} \mathbf{I}_{6 \times 6} \in \mathbb{R}^{6 \times 6}$. For the test function let $\mathbf{v}_1 \in \mathbb{R}^6$ be the largest eigenvector of $\boldsymbol{\Sigma}^{\text{LAP}}$ and set

$$f(\boldsymbol{\theta}) = 2 \cdot \mathbf{1} \{(\boldsymbol{\theta} - \boldsymbol{\mu}^{\text{LAP}}) \cdot \mathbf{v}_1 \geq 0\} - 1 \tag{28}$$

so that $f(\boldsymbol{\theta}) \in \{\pm 1\}$ for all values of $\boldsymbol{\theta}$. The idea behind this choice of test function is that the asymptotic variance of the MFIS estimator (6) is largest whenever f is not tightly concentrated around its expectation under q_{h^*} . Here the expectation of f under q_{h^*} should be close to zero even though f itself is never close to zero.

5.1.3 Results

The Laplace approximation to each surrogate posterior p_h is fit using the Newton-CG method where the gradient and Hessian matrix are computed using a second-order finite difference scheme with a total of $M_{\text{fit}} = 1150$ model evaluations at each fidelity. The cost function has the form $c(h) = c_0 + c_1/h$ and accuracy has the form $\delta(h) = O(h^2)$ since we use linear finite elements. The cost is linear in h^{-1} since the system of linear equations is tri-diagonal. We estimate the χ^2 divergence with Monte Carlo estimator

$$\hat{\chi}_{h,m}^2 = m \frac{\sum_{i=1}^m (p(\boldsymbol{\theta}^{(i)})/q_h(\boldsymbol{\theta}^{(i)}))^2}{\left(\sum_{i=1}^m p(\boldsymbol{\theta}^{(i)})/q_h(\boldsymbol{\theta}^{(i)})\right)^2} \rightarrow \chi^2(p \parallel q_h) + 1, \quad \text{almost surely as } m \rightarrow \infty \quad (29)$$

and $\{\boldsymbol{\theta}^{(i)}\}_{i=1}^m$ are i.i.d. samples drawn from q_h . Then the curve $K_0 e^{K_1 h^2}$ is fit using the estimated χ^2 values $\hat{\chi}_{h,10^3}^2$ for each fidelity $h^{-1} = 8, 12, 16, \dots, 64$ averaged over $N_1 = 500$ independent trials. The measured χ^2 values are

$$\hat{\chi}_{\text{meas},h}^2 = \frac{1}{N_1} \sum_{i=1}^{N_1} (\hat{\chi}_{h,m}^2)^{(i)}$$

with the superscript (i) denoting one of the independent trials. The fitted curve along with the measured values are shown in Figure 1. We see that the χ^2 divergence is large for low fidelities but quickly levels off and we are limited by the restriction the biasing density to be the Laplace approximation rather than the fidelity of the model.

Since we only consider finitely many surrogate models $h^{-1} = 8, 12, 16, \dots, 64$, to solve the optimization problem (16) we just use a brute force search to find the optimal pair (h^*, m^*) . Figure 1 shows the optimal fidelity as a function of the tolerance ϵ . As the tolerance shrinks we require a higher-fidelity model to fit the Laplace approximation. Using the optimal pair (h^*, m^*) , Figure 2 shows the theoretical optimal trade-off between cost in seconds and mean-squared error (MSE) of the estimator \hat{f}_{h^*, m^*} . We estimated the true value $\mathbb{E}_p[f]$ using $\hat{f}_{H,10^5}$ and averaged the results over $N_2 = 500$ independent trials (again denoted by the superscript (i))

$$\bar{f} = \frac{1}{N_2} \sum_{i=1}^{N_2} \hat{f}_{H,10^5}^{(i)}. \quad (30)$$

Next we estimated the MSE of \hat{f}_{h^*, m^*} using $N_3 = 1000$ trials

$$\widehat{\text{MSE}}_\epsilon = \frac{1}{N_3} \sum_{i=1}^{N_3} \left(\hat{f}_{h^*, m^*}^{(i)} - \bar{f} \right)^2. \quad (31)$$

Here the subscript ϵ denotes the dependence of the optimal pair (h^*, m^*) on the tolerance ϵ . Figure 2 shows the averaged MSE over $N_3 = 1000$ trials for different tolerances ϵ as well as the MSE for the estimators \hat{f}_{H, m_H} and $\hat{f}_{h_0, m_{h_0}}$ where the number of samples is

$$m_h = \frac{K_0}{\epsilon} \exp(K_1 h^2)$$

and $h_0 = 8$ is the lowest fidelity we consider (for the surrogate only estimator we average only $N_3 = 500$ trials). For moderate error tolerances we can achieve an order of magnitude speedup since most of the cost comes from fitting the Laplace approximation; using a very high-fidelity model is not necessary, but using a very cheap surrogate model is insufficient. As the tolerance shrinks, most of the computation shifts to the online sampling phase which begins to dominate and little speedup is obtained.

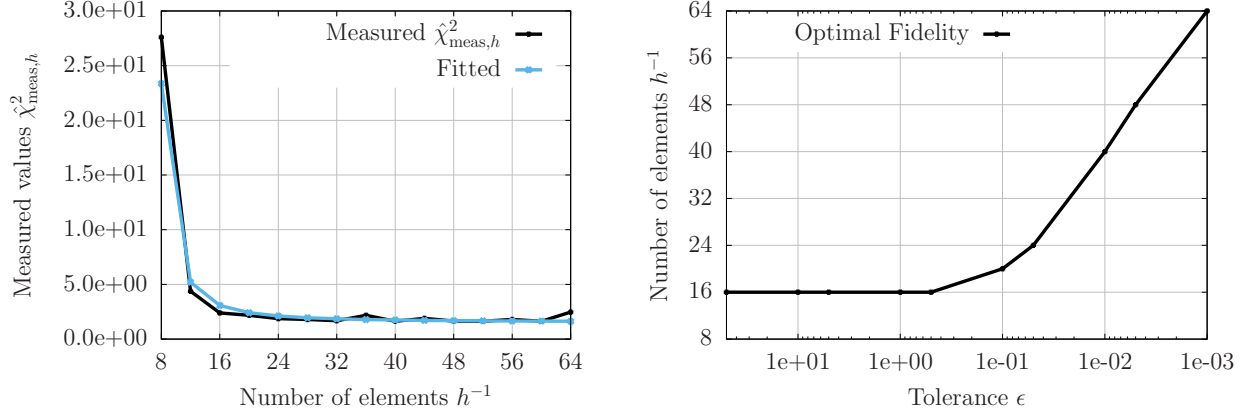


Figure 1: (Left) The measured χ^2 divergences, $\hat{\chi}_{\text{meas},h}^2$, between the high-fidelity posterior p and the Laplace approximation q_h to each surrogate posterior p_h . (Right) The optimal fidelity for the number of elements $(h^*)^{-1}$ from the optimization (16) as the tolerance ϵ on the MSE changes.

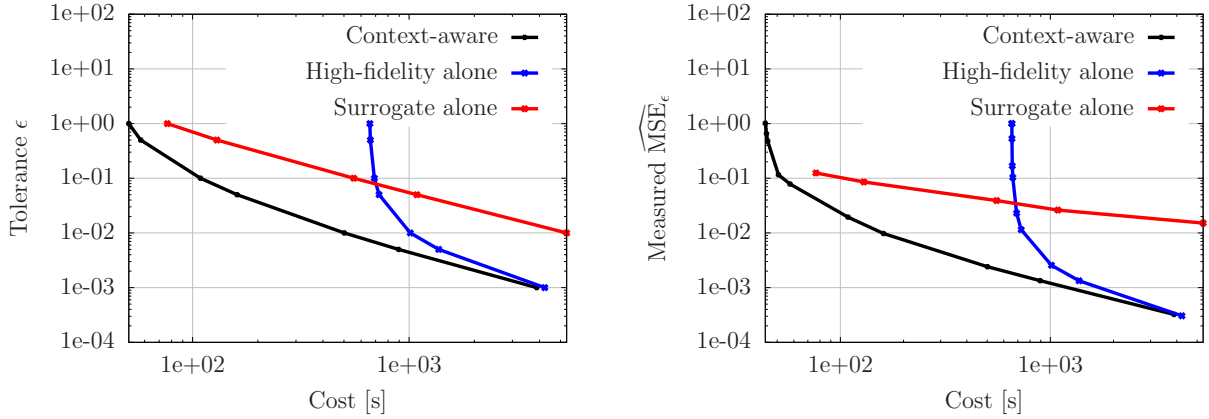


Figure 2: (Left) The theoretical error tolerance ϵ against the total cost (seconds of CPU time) to fit the Laplace approximation q_{h^*} of p_{h^*} and draw m^* samples. (Right) The actual measured $\widehat{\text{MSE}}_\epsilon$ against the total cost. Note that the results shown in the left plot is an upper bound for the results shown in right plot by the bound (3).

5.2 Euler Bernoulli Problem

In the second example we infer the effective stiffness of an Euler Bernoulli beam. The forward-model code is available on GitHub¹ and was developed by Matthew Parno as a part of the 2018 Gene Golub SIAM Summer School on “Inverse Problems: Systematic Integration of Data with Models under Uncertainty”. The rest of the setup of this problem is taken from Section 4.2 of [29].

5.2.1 Problem Setup

Let $\Omega = (0, 1) \subset \mathbb{R}$ and $\Theta = \mathbb{R}^6$ and consider the PDE

$$\frac{\partial^2}{\partial x^2} \left(E(x; \boldsymbol{\theta}) \frac{\partial^2}{\partial x^2} u(x; \boldsymbol{\theta}) \right) = f(x), \quad x \in \Omega \quad (32)$$

with boundary conditions

$$u(0; \boldsymbol{\theta}) = 0, \quad \frac{\partial u}{\partial x}(0; \boldsymbol{\theta}) = 0, \quad \frac{\partial^2 u}{\partial x^2}(1; \boldsymbol{\theta}) = 0, \quad \frac{\partial^3 u}{\partial x^3}(1; \boldsymbol{\theta}) = 0$$

where $u : \Omega \times \Theta \rightarrow \mathbb{R}$ is the displacement and $E : \Omega \times \Theta \rightarrow \mathbb{R}$ is the effective stiffness of the beam. The applied force $f(x)$ is taken to be $f(x) = 1$. The effective stiffness $E(x; \boldsymbol{\theta})$ is a smooth piecewise constant defined in the same way as the log-diffusivity (27) but with θ_i replaced by $|\theta_i|$ for $i = 1, \dots, 6$. We discretize (32) in the spatial domain Ω with a mesh width $h > 0$ (i.e. $h^{-1} + 1$ grid points) using a second-order finite difference scheme and solve the resulting linear system of equations for the discretized solution u_h at the grid points.

The parameter-to-observable map $\mathcal{F}_h : \Theta \rightarrow \mathbb{R}^{40}$ is the linear interpolant of the $h^{-1} + 1$ grid points evaluated at 40 equally spaced points in the spatial domain $(0, 1)$

$$(\mathcal{F}_h(\boldsymbol{\theta}))_i = u_h \left(\frac{i-1}{39} \right), \quad i = 1, \dots, 40$$

Note that we exclude the left end-point at $x = 0$ since it is fixed by the boundary conditions. We set the high-fidelity map to be $\mathcal{F} = \mathcal{F}_H$ with $H^{-1} + 1 = 256$ grid points and for the surrogate maps we again consider $h^{-1} + 1 = 8, 12, 16, \dots, 64$.

5.2.2 Setup of the inverse problem

A single observation $\mathbf{y} = \mathcal{F}(\boldsymbol{\theta}_{\text{truth}}) + \boldsymbol{\eta} \in \mathbb{R}^{40}$ is generated where $\boldsymbol{\theta}_{\text{truth}} = (1, \dots, 1)^T \in \mathbb{R}^6$ and $\boldsymbol{\eta} \sim N(\mathbf{0}, \boldsymbol{\Gamma})$ with noise covariance $\boldsymbol{\Gamma} = 5.623 \times 10^{-4} \mathbf{I}_{40 \times 40}$. The added noise now corresponds to approximately 5% of the true solution u at the right endpoint $x = 1$. The prior is again a Gaussian with mean $\boldsymbol{\mu}_{\text{pr}} = (1, \dots, 1)^T \in \mathbb{R}^6$ and covariance $\boldsymbol{\Sigma}_{\text{pr}} = 1.778 \times 10^{-2} \mathbf{I}_{6 \times 6} \in \mathbb{R}^{6 \times 6}$. For the test function we use the same test function (28) from the steady-state heat problem.

5.2.3 Results

We again fit the Laplace approximation to each surrogate posterior p_h using Newton-CG with the gradient and Hessian computed by second-order finite difference approximations. The total number of model evaluations is $M_{\text{fit}} = 1800$ at each fidelity. The cost function has the form $c(h) = c_0 + c_1/h$ (linear in h^{-1} because the system of linear equations from the discretization is sparse) and the surrogate accuracy has the form $\delta(h) = O(h^2)$ from the second-order finite difference spatial discretization.

¹<https://github.com/g2s3-2018/labs>

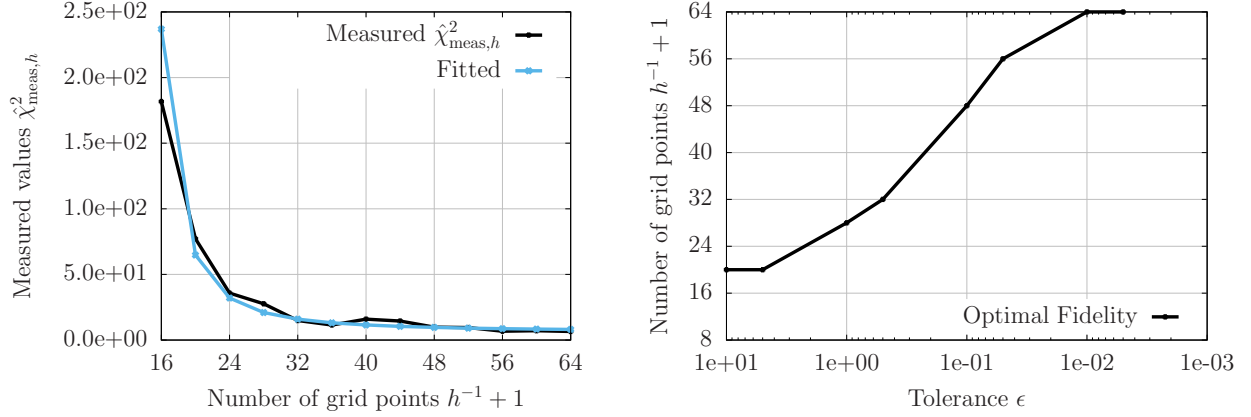


Figure 3: (Left) The measured χ^2 divergences, $\hat{\chi}_{\text{meas},h}^2$, between the high-fidelity posterior p and the Laplace approximation q_h to each surrogate posterior p_h . (Right) The optimal fidelity for the number of grid points $(h^*)^{-1} + 1$ from the optimization (16) as the tolerance ϵ on the MSE changes.

We use the χ^2 divergence estimator $\hat{\chi}_{h,10^5}^2$ from (29) and average the results over $N_1 = 100$ independent trials to obtain the measured value $\hat{\chi}_{\text{meas},h}^2$ as in (29) for each surrogate map $h^{-1} + 1 = 8, 12, 16 \dots, 64$. We then use these measured values to fit the curve $K_0 e^{K_1 h^2}$. Figure 3 shows the results. Observe that the χ^2 divergence quickly levels off again.

The optimal pair (h^*, m^*) to (16) is found using a brute-force search and Figure 3 shows the optimal number of grid points $(h^*)^{-1} + 1$ as a function of the MSE tolerance ϵ . When the tolerance is too small the optimal fidelity is actually the high-fidelity since we do not consider any surrogate models with $h^{-1} + 1$ between 64 and 256. Figure 4 shows the theoretical optimal cost and error trade-off for \hat{f}_{h^*, m^*} . We estimated the true value $\mathbb{E}_p[f]$ using $\hat{f}_{H,10^5}$ with $N_2 = 100$ independent trials using equation (30) and the MSE was estimated with $N_3 = 2500$ independent trials using equation (31). Here the lowest-fidelity surrogate model corresponds to $h_0 = 16$. From the plot we can observe an order of magnitude speedup for moderate tolerances where we do not need to use a high-fidelity model to fit the Laplace approximation. Also note that the theoretical trade-off is an upper bound but the shape matches closely with the measured results.

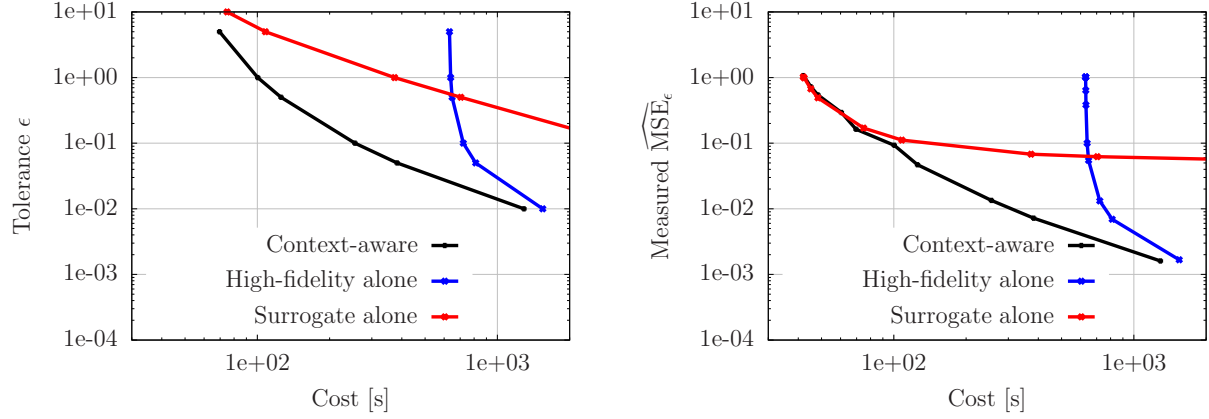


Figure 4: (Left) The theoretical error tolerance ϵ against the total cost (seconds of CPU time) to fit the Laplace approximation q_{h^*} of p_{h^*} and draw m^* samples. (Right) The actual measured \widehat{MSE}_ϵ against the total cost. Note that the results in the left plot are upper bounding the results in the right plot by the bound (3).

Acknowledgements

The authors acknowledge support of the National Science Foundation under Grant No. 1761068 and Grant No. 1901091. The first author was supported in part by the Research Training Group in Modeling and Simulation funded by the National Science Foundation via grant RTG/DMS – 1646339. The second author also acknowledges support of the AFOSR MURI on multi-information sources of multi-physics systems under Award Number FA9550-15-1-0038 (Dr. Fariba Fahroo).

References

- [1] S. Agapiou, O. Papaspiliopoulos, D. Sanz-Alonso, and A. Stuart. Importance sampling: Intrinsic dimension and computational cost. *Statist. Sci.*, 32(3):405–431, 2017.
- [2] A. Antoulas. *Approximation of Large-Scale Dynamical Systems*. Advances in Design and Control. SIAM, 2005.
- [3] P. Benner, S. Gugercin, and K. Willcox. A survey of projection-based model reduction for parametric dynamical systems. *SIAM Rev.*, 57(4):483–531, 2015.
- [4] S. Brenner and R. Scott. *The Mathematical Theory of Finite Element Methods*. Texts in Applied Mathematics. Springer-Verlag New York, 2008.
- [5] Y. Cao, M. Gunzburger, F. Hua, and X. Wang. Analysis and finite element approximation of a coupled, continuum pipe-flow/Darcy model for flow in porous media with embedded conduits. *Numerical Methods Partial Differential Equations*, 27:1242–1252, 2011.
- [6] S. Chatterjee and P. Diaconis. The sample size required in importance sampling. *Ann. Appl. Probab.*, 28(2):1099–1135, 2018.
- [7] P. Chen and A. Quarteroni. Accurate and efficient evaluation of failure probability for partial differential equations with random input data. *Computer Methods in Applied Mechanics and Engineering*, 267:233–260, 2013.

- [8] P. Chen, A. Quarteroni, and G. Rozza. Reduced basis methods for uncertainty quantification. *SIAM/ASA J. Uncertain. Quantif.*, 5:813–869, 2017.
- [9] T. Cui, Y. M. Marzouk, and K. E. Willcox. Data-driven model reduction for the Bayesian solution of inverse problems. *International Journal for Numerical Methods in Engineering*, 102(5):966–990, 2015.
- [10] A. Davis, Y. Marzouk, A. Smith, and N. Pillai. Rate-optimal refinement strategies for local approximation MCMC. *arXiv*, 2006.00032, 2020.
- [11] G. P. Dehaene. Computing the quality of the Laplace approximation. In *Neural Information Processing Systems*, 2017.
- [12] G. Detommaso, T. Dodwell, and R. Scheichl. Continuous level Monte Carlo and sample-adaptive model hierarchies. *SIAM/ASA Journal on Uncertainty Quantification*, 7(1):93–116, 2019.
- [13] I.-G. Farcas. *Context-aware Model Hierarchies for Higher-dimensional Uncertainty Quantification*. Dissertation, Technische Universität München, München, 2020.
- [14] A. Forrester and A. Keane. Recent advances in surrogate-based optimization. *Progr. Aerosp. Sci.*, 45:50–79, 2009.
- [15] M. Heinkenschloss, B. Kramer, and T. Takhtaganov. Adaptive reduced-order model construction for conditional value-at-risk estimation. *SIAM/ASA Journal on Uncertainty Quantification*, 8(2):668–692, 2020.
- [16] M. Heinkenschloss, B. Kramer, T. Takhtaganov, and K. Willcox. Conditional-value-at-risk estimation via reduced-order models. *SIAM/ASA Journal on Uncertainty Quantification*, 6(4):1395–1423, 2018.
- [17] J. S. Hesthaven, G. Rozza, and B. Stamm. *Certified Reduced Basis Methods for Parametrized Partial Differential Equations*. SpringerBriefs in Mathematics. Springer International Publishing, 2016.
- [18] H. Hoel, E. von Schwerin, A. Szepessy, and R. Tempone. Adaptive multilevel Monte Carlo simulation. In B. Engquist, O. Runborg, and Y.-H. R. Tsai, editors, *Numerical Analysis of Multiscale Computations*, pages 217–234, Berlin, Heidelberg, 2012. Springer Berlin Heidelberg.
- [19] H. Hoel, E. von Schwerin, A. Szepessy, and R. Tempone. Implementation and analysis of an adaptive multilevel Monte Carlo algorithm. *Monte Carlo Methods and Applications*, 20(1):1 – 41, 2014.
- [20] J. Lang, R. Scheichl, and D. Silvester. A fully adaptive multilevel stochastic collocation strategy for solving elliptic PDEs with random data. *Journal of Computational Physics*, 419:109692, 2020.
- [21] R. J. LeVeque. *Finite Difference Methods for Ordinary and Partial Differential Equations: Steady-State and Time-Dependent Problems*. SIAM, 2007.
- [22] J. Li, J. Li, and D. Xiu. An efficient surrogate-based method for computing rare failure probability. *Journal of Computational Physics*, 230(24):8683–8697, 2011.
- [23] J. Li and D. Xiu. Evaluation of failure probability via surrogate models. *Journal of Computational Physics*, 229(3):8966–8980, 2010.
- [24] A. J. Majda and G. Gershgorin. Quantifying uncertainty in climate change science through empirical information theory. *Proceedings of the National Academy of Sciences of the United States of America*, 107(34):14958–14963, 2010.
- [25] A. Narayan, C. Gittelson, and D. Xiu. A stochastic collocation algorithm with multifidelity models. *SIAM J. Sci. Comput.*, 36:495–521, 2014.

- [26] L. W. Ng and K. Willcox. Monte-Carlo information-reuse approach to aircraft conceptual design optimization under uncertainty. *Journal of Aircraft*, 53:427–438, 2016.
- [27] B. Peherstorfer. Multifidelity Monte Carlo estimation with adaptive low-fidelity models. *SIAM/ASA Journal on Uncertainty Quantification*, 7:579–603, 2019.
- [28] B. Peherstorfer, T. Cui, Y. Marzouk, and K. Willcox. Multifidelity importance sampling. *Computer Methods in Applied Mechanics and Engineering*, 300:490–509, 2016.
- [29] B. Peherstorfer and Y. Marzouk. A transport-based multifidelity preconditioner for Markov chain Monte Carlo. *Advances in Computational Mathematics*, 45:2321–2348, 2019.
- [30] B. Peherstorfer, K. Willcox, and M. Gunzburger. Survey of multifidelity methods in uncertainty propagation, inference, and optimization. *SIAM Review*, 60(3):550–591, 2018.
- [31] A. Quarteroni, G. Rozza, and A. Manzoni. Certified reduced basis approximation for parametrized partial differential equations and applications. *Journal of Mathematics in Industry*, 1(1):1–49, 2011.
- [32] C. Rasmussen and C. Williams. *Gaussian Processes for Machine Learning*. MIT Press, 2016.
- [33] D. Sanz-Alonso. Importance sampling and necessary sample size: An information theory approach. *SIAM/ASA J. Uncertainty Quantification*, 6(2):867–879, 2018.
- [34] C. Schillings, B. Sprungk, and P. Wacker. On the convergence of the Laplace approximation and noise-level-robustness of Laplace-based Monte Carlo methods for Bayesian inverse problems. *Numer. Math.*, 145:915–971, 2020.
- [35] A. Stuart. Inverse problems: A Bayesian perspective. *Acta Numerica*, 19:451–559, 2010.
- [36] T. Sullivan. *Introduction to Uncertainty Quantification*. Springer, 2015.
- [37] A. B. Tsybakov. *Introduction to Nonparametric Estimation*. Springer Series in Statistics. Springer, 2009.
- [38] R. Vershynin. *High-dimensional probability: an introduction with applications in data science*. Cambridge University Press, 2018.